

Surface-Assisted Transient Displacement Charge Technique. II. Effect of Gases on Photoinduced Charge Transfer in Self-Assembled Monolayers

Alexey V. Krasnoslobodtsev and Sergei N. Smirnov*

Department of Chemistry and Biochemistry, New Mexico State University, Las Cruces, New Mexico 88003

Received: February 5, 2006; In Final Form: July 17, 2006

Surface-assisted photoinduced transient displacement charge (SPTDC) technique was used to study charge transfer in self-assembled monolayers of 7-diethylaminocoumarin covalently linked to an oxide surface in the atmosphere of different gases. The dipole signal was found to be opposite to that in solution and dependent on the nature of the gas and its pressure. The results were explained by collision-induced relaxation that impedes uninhibited tilting of molecules onto the surface. Collisions with paramagnetic oxygen induce intersystem crossing to long-lived triplet dipolar states of coumarin with the rate close to half of that for the collision rate.

Introduction

As was shown in the preceding article, the surface-assisted transient displacement charge technique, or SPTDC, allows direct measurements of the dipole moment change upon photoexcitation in molecules covalently bound to the surface.¹ The photoinduced voltage, v , arises due to the dipole moment change in molecules oriented by the surface, as illustrated in Figure 1 by arrows. The signal had different signs for molecules with dipole moments oriented oppositely with respect to the surface, in accordance with the directions of charge shift in them upon photoexcitation. The average orientation of molecules in a monolayer, as evaluated by linear dichroism,^{2–4} depended on solvent polarity, with increasing preference toward orientation parallel to the surface in nonpolar solvents. The dipole signal amplitude followed this trend but declined much faster in low-polarity solvents.¹ Solvent-free monolayer films showed even greater tendency for orienting molecules parallel to the surface.³

In this paper, we describe the results of photoinduced transient displacement charge (SPTDC) measurements of the dipole signal in self-assembled monolayers (SAM) of 7-diethylaminocoumarin in the atmosphere of different gases. The dipole signal appeared opposite in sign to that in solution, and the amplitude of the dipole signal varied with the type of gas and pressure. As shown below, the effect is due to the collision-induced relaxation, which prevents molecules from uninhibited tilting onto the surface. Collisions with paramagnetic oxygen induce intersystem crossing in coumarin SAM and yield long-lived triplet dipolar states.

Experimental Section

7-Diethylaminocoumarin-3-carboxylic acid succinimidyl ester (commercial name D-1412, coumarin A), from Molecular Probes, and coumarin 460, from Exciton, Inc., were used without purification. Substrates: mica and polished quartz slides (12 mm \times 25 mm \times 0.3 mm) from Quartz International, were modified with trimethoxyaminosilanes (3-amino-propyltrimethoxysilane, from Aldrich), and then stained by a dye on one side to form a self-assembled monolayer (SAM) using the

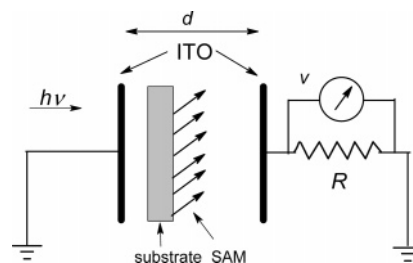


Figure 1. Schematic representation of the surface-assisted photoinduced transient displacement charge (SPTDC) setup.

previously described procedure.^{2,3} Quartz slides were first cleaned in 0.1 N NaOH, then in 1:1 MeOH/HCl, heated for 2 h in concentrated H₂SO₄, and rinsed in a copious amount of deionized (DI) water. Immediately prior to silanization, the slides were boiled in DI water, rinsed in acetone, and dried at 100 °C. In the case of mica, the upper layer was peeled off prior to use, followed by boiling in DI water and drying. Cleaned slides were silanized from 2% v/v acetone solution of trimethoxyaminosilane, washed with acetone, and baked at 100 °C in an oven for 5 min.

The staining of the silanized slides by coumarin A was performed only on one side of a substrate. This was done by placing a drop of 0.6 mM DMSO dye solution between the slide and the surface of a Petri dish. The stained slides were washed in acetone and dried in an oven at ca. 100 °C. No noticeable deterioration of the surface concentration of dye molecules was observed within a month after staining when stored under dark, dry conditions or in organic solvents.

The setup for surface-assisted PTDC (SPTDC) technique was described before.¹ Two excitation sources were used: either the third harmonic from a Nd:YAG laser (“Orion SB-R” from MPB) Raman shifted on H₂, CH₄, or CF₄ (to make 416, 396, or 366 nm, respectively) or a VSL-337 nitrogen laser (337 nm). The laser pulse durations were 20 ps and 4 ns, respectively. The dipole signal was measured across the 20 kΩ input resistance of a P6249 high-impedance probe (4 GHz), also from Tektronix. The ITO cell with a 3 mm gap was encased into a brass chamber with quartz windows to allow for the exchange of gas and variation of its pressure. Stray capacitance of the cell, C_s , was

* Corresponding author. E-mail: snsm@nmsu.edu.

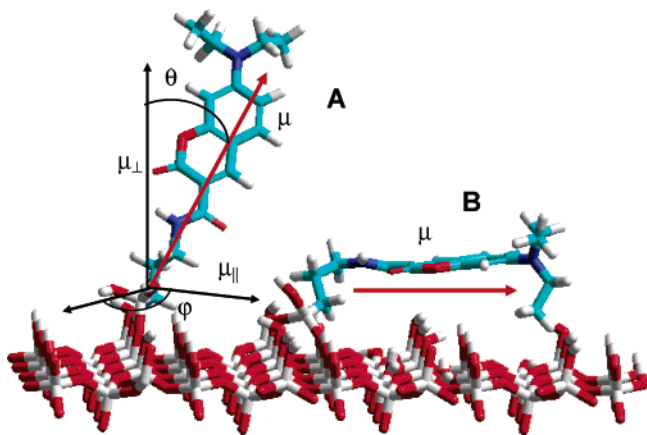


Figure 2. Illustration of the Eulerian angles, θ and φ , for a molecule on the surface. Two possible orientations, A and B, for covalently linked coumarin molecules on mica are shown. Orientation B was obtained by MM+ energy minimization of the molecule on the surface and demonstrates that the maximum value of θ does not exceed 90° .

measured to be ca. 4.3 pF, comparable with that of the cell itself. The latter is calculated from the cell dimensions and the portion of its volume filled with substrate material (quartz or mica). A possible systematic error in evaluating the latter would contribute identically to all the resulting signals. Measurements in different gases were repeated on the same samples; therefore, the ratio between the dipole signal amplitudes was unaffected. As it will also be discussed later, experimentally measured RC time is close to that calculated with the above-mentioned procedure, thus corroborating its accuracy.

Results and Discussion.

Following the theory developed in the preceding article,¹ one can use eq 1 to evaluate the dipole signal, v :

$$v + \tau_{RC} \frac{dv}{dt} = RS \frac{d}{dt} (\langle \mu_{\perp} \rangle N) \quad (1)$$

where S is the electrode area, and R is the load resistor. The number of excited dipoles on the surface, N , can be calculated from the absorbed energy. In the charge displacement limit (i.e., with large τ_{RC}) after integration over time, eq 1 transforms into:

$$v = \frac{RS}{\tau_{RC}} (\langle \Delta \mu_{\perp} \rangle N) \quad (2)$$

where the RC time, τ_{RC} , includes contributions from the cell's capacitance and stray capacitance, C_s :

$$\tau_{RC} = R(\epsilon \epsilon_0 S/d + C_s) \quad (3)$$

Here, the cell capacitance is calculated from the electrode area, the gap distance, d , between them, and the dielectric constant, ϵ , of the solvent inside.

The average perpendicular projection of the dipole moment change, $\langle \Delta \mu_{\perp} \rangle$, is the difference between averaged perpendicular projections of the excited, $\mu_{exc} \langle \cos \theta \rangle_{exc}$, and the depleted ground-state, $\mu_g \langle \cos \theta \rangle_g$, dipole moments:

$$\langle \Delta \mu_{\perp} \rangle = \mu_{exc} \langle \cos \theta \rangle_{exc} - \mu_g \langle \cos \theta \rangle_g = \mu_{exc} \int f_{exc}(\theta) \cos \theta d\Omega - \mu_g \int f_g(\theta) \cos \theta d\Omega \quad (4)$$

where θ is the angle between the direction of the dipole moment and the axis perpendicular to the surface (see Figure 2). If the transition moment is parallel to both dipole moments, the ground

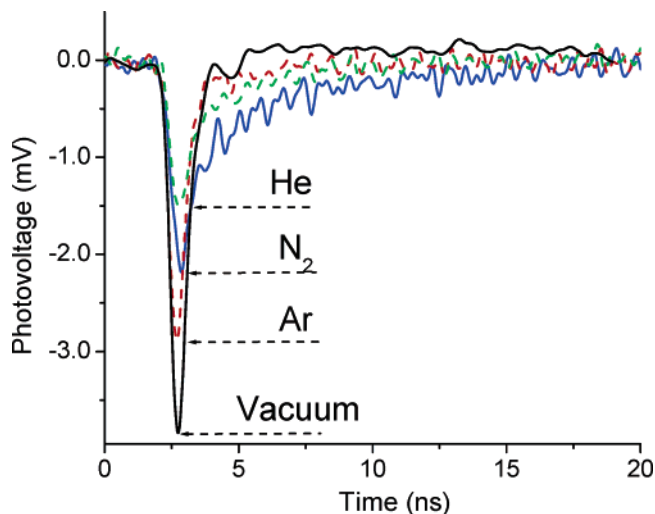


Figure 3. SPTDC dipole signals for coumarin SAM immobilized on one side of quartz slides stacked in one direction. Signals in different gaseous media are normalized to the same absorbed energy, 7 μJ , at the excitation wavelength, 396 nm.

TABLE 1: Fitting Parameters for SPTDC Dipole Signal of Coumarin for Different Gases

	vacuum	Ar	O ₂	N ₂	He
$\langle \Delta \mu_{\perp} \rangle_{\text{max}}$, D	-3.0	-1.9	-1.5	-1.5	-0.9
τ_F , ns ^a	0.2	0.2	0.4 ^c	0.4	0.4
τ_{col} , ns ^b	∞	0.93	0.83	0.78	0.29

^a lifetime of singlet state. ^b Collision time constant with the surface-bound molecules estimated using eq 7 at atmospheric pressure (670 Torr).

and excited states (a good approximation for coumarin), and no rotation takes place, the angular distribution functions, $f_{exc}(\theta)$ and $f_g(\theta)$, can be taken as identical and equal to the distribution of excited molecules. In that case, $\langle \Delta \mu_{\perp} \rangle$ can be directly related to the change in dipole moment, $\Delta \mu = \mu_{exc} - \mu_g$, and the probability of excitation, $P(\theta)$.¹ For a uniform distribution on a hemisphere when the laser excitation is perpendicular to the surface, the following simple formula of the "static" pseudouniform $\langle \Delta \mu_{\perp} \rangle_{\text{static}}$ can be derived:¹

$$\langle \Delta \mu_{\perp} \rangle_{\text{static}} = (\mu_{exc} - \mu_g) \int P(\theta) \cos \theta d\Omega = \frac{3}{8} (\mu_{exc} - \mu_g) = \frac{3}{8} \Delta \mu \quad (5)$$

Experimentally observed values of $\langle \Delta \mu_{\perp} \rangle$ for covalently immobilized coumarin appeared to be close to the value obtained using eq 1 only in highly polar solvents, but declined with decreasing solvent polarity.¹ This trend correlates with the optical absorption observations: coumarin has a greater degree of orientation parallel to the surface in low-polarity solvent,¹ but $\langle \Delta \mu_{\perp} \rangle$ dependence on solvent polarity was much more dramatic; $\langle \Delta \mu_{\perp} \rangle$ dropped from 1.1 D in ethanol to ~ 0.07 D in hexane.¹

A much greater "discrepancy" was observed for the dipole signal of surface-bound coumarin measured in gaseous media; the signals were negative (opposite to those in solution) and dependent on the gas. Figure 3 and Table 1 illustrate this behavior. The polarity of the signal should be defined by the direction of charge separation in a monolayer (direction of the dipole moment change), and grasping why the signal flips in the gas phase was difficult at first. One can offer a number of possible explanations for the phenomenon, and we will address them all below.

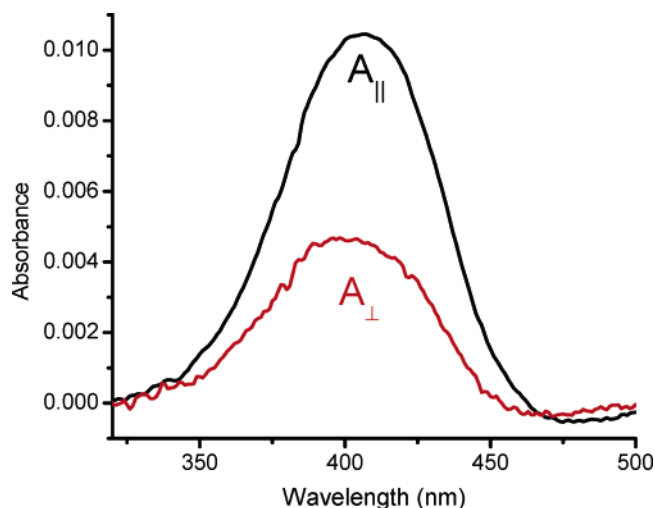


Figure 4. UV absorption spectra of coumarin SAM on quartz for parallel, $A_{||}$, and perpendicular, A_{\perp} , polarizations with respect to the surface.

Can the static orientation of surface-bound molecules without solvent be opposite to that in liquid solvents? After all, there is a tendency for decreasing perpendicular-to-the-surface orientation for the ground-state coumarin in low-polarity solvents.² It is even greater in the gas phase.³ As Figure 4 illustrates, the average projection, $\langle \cos^2 \theta \rangle$, calculated from the absorption intensities parallel, $A_{||}$, and perpendicular, A_{\perp} , to the surface:^{2,3}

$$\langle \cos^2 \theta \rangle = \frac{A_{\perp}}{2A_{||} + A_{\perp}} \quad (6)$$

is much lower in the gas phase ($\langle \cos^2 \theta \rangle = 0.18$) than in any solvent. If the distribution were reduced to a single angle, θ_{av} , that angle would be almost 65° from the normal to the surface. Experiments with a noncovalently immobilized similar molecule, coumarin 460, which was spread from ethanol solution on the surface and dried, also showed a negative dipole signal of similar amplitude. Thus, one could speculate that there is a tendency of attractive interaction between coumarins and the surface, likely in the form of amine–hydroxyl hydrogen bonding. If the linker's length and the surface roughness (as little as a few Å) could provide sufficient room and flexibility, coumarin molecules would relax to the lowest energy orientation/conformation with aminogroups pointing toward the surface and provide an opposite dipole orientation. To eliminate this option, coumarin was covalently immobilized on an atomically flat mica surface. The negative dipole signal was also observed in this case of almost identical amplitude. At the same time, molecular mechanics simulations⁵ showed that, with this linker, no opposite orientation of coumarin dipole moment was feasible for any conformation. As Figure 2 illustrates, the largest angle, θ , did not exceed 90° . Because the densities of molecules do not exceed the density of surface hydroxyls, involvement of polymeric silanes (and thus more flexible tails for coumarins) is excluded. Thus, although we have to conclude that the attractive interaction of coumarin with the surface exists and can provide means for orienting noncovalently bound molecules, it is incapable for orienting covalently attached coumarin oppositely to the surface when the short aminopropyltrimethoxysilane linker is used.

Because semiempirical calculations have no indication of any excited state with the dipole moment smaller or opposite to that of the ground state¹ and the ground-state dipole cannot

orient oppositely on the surface, a negative dipole signal for nonrotating molecules should be excluded. Instead, tilting (rotation) of dipoles after excitation should be responsible for the observed phenomenon. Figure 5 offers scenarios for different stages in dipole evolution after excitation (Figure 5B). Dipole moment reorientation can proceed through a physical tilting of the excited dipolar molecule (Figure 5C) and probably its surrounding molecules (Figure 5C'). An alternative mechanism involves no physical rotation, but energy transfers to neighboring molecules until there is eventual localization of excited energy on molecules of lower energy conformations with their dipole moments oriented more parallel to the surface (Figure 5D). Both contributions are significant, but only physical rotation/tilting can explain the negative dipole signal.

Fluorescence spectra and kinetics observed in solutions suggest¹ that the excited states have strong interaction with neighboring ground-state molecules and with other excited coumarins. Stimulated emission depends on dipole orientation and was significantly shortened under the experimental conditions. Excited coumarins oriented parallel to the surface survived for a longer time than the perpendicular ones because of a smaller dipole–dipole interaction in the latter case.¹ Fluorescence measurements without a solvent were not feasible, but the general conclusion about the correlation between dipole orientation and their excited-state lifetime should remain. In light of this mechanism, one may expect that energy transfer would assist the prevalence of surviving excited dipoles oriented parallel to the surface without their physical reorientation. This type of reorientation minimizes the overall perpendicular dipole projection caused by excitation but not lower than the ground-state value and thus cannot explain the negative going signal.

There are a number of facts corroborating that orientation of dipoles with respect to the surface is not rigid. It includes the solvent dependence of absorption^{1–3} and AFM measurements of contact potential for these monolayer films.¹⁴ In the latter method, we observed that the dipole moments of covalently linked coumarin could be oriented by an external electric field. This field should be quite high to make a significant effect, and a conductive AFM cantilever can provide such an opportunity. In the measurements of contact potential built from molecular dipoles covalently linked to the surface of ITO, the amplitudes and signs of the contact potential correlated with dipole moments and orientations for different molecules. At large distances from the surface, the contact potential was constant but dropped abruptly at short distances, where the electric field from conductive AFM tip, E , becomes sufficient to reorient dipoles, i.e. when $\mu E \sim k_B T$.¹⁴

Absorption spectra show dependence on solvent and surface concentration of covalently bound coumarin.^{2,3} Upon lowering concentration, the absorption maxima shifted to the blue, especially for the perpendicular orientation, the widths of absorption narrowed, and the anisotropy declined ($\langle \cos^2 \theta \rangle$ became closer to the value for random orientation, 0.33). This corroborates the significance of intermolecular dipole–dipole interaction. The energy of dipole–dipole interaction, E_{d-d} , depends on the magnitudes of interacting dipole moments, μ_1 and μ_2 , the separation distance between them, R , and their mutual orientation:

$$E_{d-d} = \frac{\vec{\mu}_1 \cdot \vec{\mu}_2}{R^3} - \frac{3(\vec{\mu}_1 \cdot \vec{R})(\vec{\mu}_2 \cdot \vec{R})}{R^5} \quad (7)$$

Because of the high surface densities, $N/S = 2\text{--}4 \times 10^{14} \text{ cm}^{-2}$, intermolecular separations are fairly small ($R \sim 5\text{--}7 \text{ Å}$)

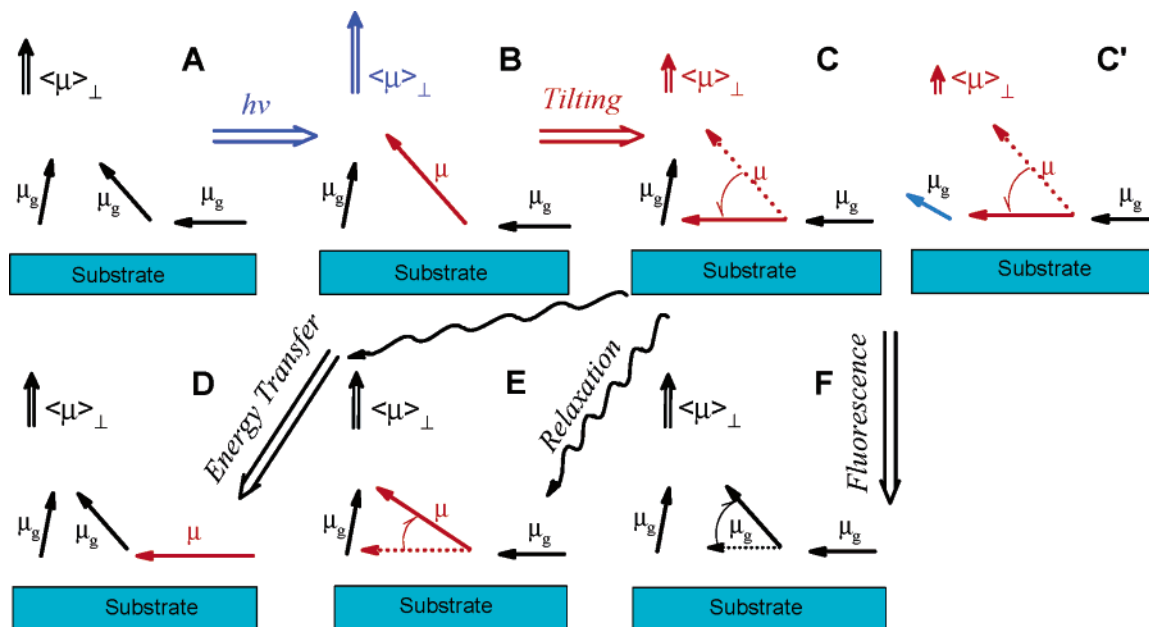


Figure 5. Illustration of different stages in evolution of dipoles on surface: A, all ground states, μ_g ; B, initial situation right after the excitation with one dipole in the excited state, μ (without changing its orientation); the average perpendicular dipole projection, $\langle\mu\rangle_\perp$, transiently increases; C, after rotation of μ , the averaged $\langle\mu\rangle_\perp$ declines below the ground-state value; C', the same as C, but some μ_g also rotate, allowing a greater decline of $\langle\mu\rangle_\perp$; D, illustration that energy transfer does not lead to a decline of $\langle\mu\rangle_\perp$; E, relaxation to the ground state via fluorescence or nonradiatively leads to recovering of $\langle\mu\rangle_\perp$ to its ground-state value; rotational (E) or energy transfer assisted (D) relaxation of μ also leads to recovery of $\langle\mu\rangle_\perp$ to its ground-state value.

and the interaction becomes significant. For two molecules with dipole moments of the ground state of coumarin, $\mu_g = 7$ D, oriented perpendicular to the surface and separated by 5 Å, their repulsive interaction, $E_{d-d} \sim 0.25$ eV, is an order of magnitude greater than $k_B T$. Similarly, when laying on the surface, the dipoles can arrange toward the lower energy attractive orientation of a similar but negative E_{d-d} value. This angular dependence of interaction is the driving force for tilting dipoles parallel to the surface. The interaction is significantly reduced in polar solvents due to the dielectric screening and makes dipoles more randomly oriented. Upon photoexcitation, when the dipole moment instantly increases by as much as 3 D (or more), the driving force to “tilt” the excited dipole, as well as its neighboring ground-state dipoles, gains an additional boost from the enhanced dipole–dipole interaction, especially when no solvent is present. One would expect that an excess energy brought during relaxation of molecules may contribute to the tilting rate but it did not; within the experimental accuracy, the signal magnitude was the same (when normalized by the absorbed energy) for excitation at the maximum, 396 nm, and at the red wing of absorption, 416 nm.

The dipole signal dependence on the nature of gas is strong evidence that static orientation of molecules cannot explain the negative dipole signal, and more importantly, it suggests that physical reorientation of molecules after excitation is the defining factor. As one can see from Figure 3, the dipole signals measured in various gaseous media (helium, nitrogen, argon) at atmospheric pressure as well as under vacuum, had negative signs but different signal amplitudes. The effect of medium on the dipole signal has no hysteresis; its sign and amplitude restored after changing solvents or drying the substrates and changing the gas during the experiment. At the same time, the absorption spectra were identical within the experimental accuracy for all gases. The amplitude of the dipole signal was the highest in vacuum and decreased in gases. Interestingly enough, the average time between collisions at ambient conditions (670 Torr in Las Cruces) is comparable with the lifetime

of coumarin’s excited state. Also, the rate of collisions between the gas molecules and the surface increases in the same order as the decline of the dipole signal, as shown in Figure 6A. The time between collisions was calculated using eq 8:

$$\tau_{\text{col}} = \frac{4}{nv_T s} = \frac{1}{ns} \sqrt{\frac{2\pi m}{k_B T}} \quad (8)$$

where s is the area occupied by one coumarin molecule, n is the number density of gaseous molecules, m and v_T are their mass and mean speed, respectively. Taking $s = 50$ Å², which is equal to the area of a coumarin molecule laying down flat on the surface (coincidentally equals the area per molecule for the typical surface coverage density of coumarin, 2×10^{14} cm⁻²) and $n = 2.2 \times 10^{19}$ cm⁻³ (at 670 Torr), one calculates τ_{col} that are given in Table 2 and in Figure 6A. Variation of the collision frequency can be achieved also by changing the gas pressure, which was performed with N₂ gas at room temperature (Figure 6B). Again, increasing frequency of collisions this way caused the dipole signal amplitude to decrease as well.

All of these are indications that some relaxation process is involved in the signal evolution. Let us describe the phenomenon by introducing three characteristic times in the dipole signal evolution: the time required for the negative dipole signal to build up via excited dipole tilting, τ_t , the orientation relaxation time, τ , and the excited-state lifetime, τ_F . We cannot claim that “tilting” is an exponential process, but it is convenient for initial consideration. We chose a name “tilting” rather than rotation to emphasize that it is different from the rotational diffusion time typically measured in PTDC technique.^{12,13} This is not only because the rotation of a molecule linked to the surface takes place without any solvent and the surrounding highly dipolar molecules are similarly hindered in their movement, but primarily because this tilting is a “directed” motion that can be interrupted by relaxation processes such as collision with gas. Below, we will discuss the meaning of these parameters, their

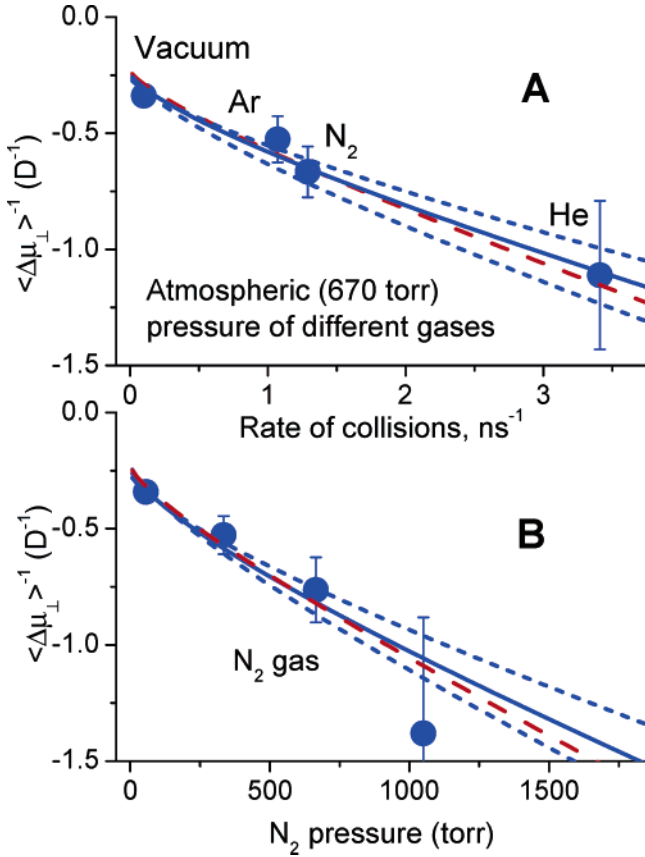


Figure 6. Dependence of the average dipole moment projection change on the collision rate for different gases at 670 Torr (A) and for nitrogen as a function of pressure (B). Collision rates are calculated using eq 7, with the area of coumarin molecule $s = 50 \text{ \AA}^2$. The solid curves represent the best fits using eq 12 with the same $\langle \Delta\mu_{\perp} \rangle_e = 5.7 \pm 1.2$, and $\mu/\mu_g = 1.4$ but different tilting: $\xi\tau_t = 1.2 \pm 0.2 \text{ ns}$ and $0.6 \pm 0.15 \text{ ns}$ for A and B, respectively; the dashed curves are those for the parameters on the limits. The red dashed curves show best fits using $\mu/\mu_g = 1.0$ and $\langle \Delta\mu_{\perp} \rangle_e = 4.3 \text{ D}$ with the same values of $\xi\tau_t = 1.2$ and 0.6 ns .

effect on the dipole signal, and the role of collisions with gaseous molecules.

These three characteristic times capture the main features of the process. One can describe the evolution of the average perpendicular dipole moment projection, $\langle \Delta\mu_{\perp} \rangle$, as built up on competition between the “exponential” tilting toward the maximum amplitude value, $-\langle \Delta\mu_{\perp} \rangle_{\text{max}}$, with a time constant τ_t , and relaxation to zero with an effective time, τ . In this phenomenological model, the effective relaxation time is a geometrical mean of the “native” relaxation time, τ_r , and the collision-induced relaxation time, τ_{col} :

$$\frac{1}{\tau} = \frac{\xi}{\tau_{\text{col}}} + \frac{1}{\tau_r} = \xi k_{\text{col}} n + \frac{1}{\tau_r} \quad (9)$$

The collision efficiency factor, ξ , was introduced here to scale down the rate of relaxation, which can be less than the collision rate with gaseous molecules. The rate constant of collisions, k_{col} , can be calculated similarly to eq 8, as:

$$k_{\text{col}} = \frac{v_T}{4s} \quad (10)$$

where s is the area occupied by one coumarin molecule and v_T is the average thermal velocity of gaseous molecules.

TABLE 2: Kinetic Parameters Used for SPTDC Dipole Signal Fitting of Coumarin in Air and O₂

	coumarin B		coumarin 460	
	oxygen	air	oxygen	air
τ_F, ns^a	0.4		4.3	
$\tau_{\text{isc}}, \text{ns}^b$	2.4 ± 1	14 ± 2	2.4 ± 1	14 ± 2
$\tau_{\text{col}}, \text{ns}^c$	0.83	3.95	0.83	3.95

^a Lifetime of the singlet state; presumed to be independent of partial pressure of O₂. ^b Intersystem crossing time from the fittings. ^c Collision time of O₂ with the surface-bound molecules estimated using eq 7 and partial pressure of O₂ = 670 and 140 Torr for pure oxygen and air, respectively, and given for comparison.

This competition between tilting and relaxation results in double-exponential growth/decay kinetics:

$$\langle \Delta\mu_{\perp} \rangle(t) = -\langle \mu_{\perp} \rangle_g \exp(-t/\tau) - \frac{\langle \mu_{\perp} \rangle_e}{\tau_t - \tau} [\tau_t \exp(-t/\tau) - \tau \exp(-t/\tau_t)] \quad (11)$$

where $\langle \Delta\mu_{\perp} \rangle_g$ is the equilibrium polarization of the ground-state dipoles and $\langle \Delta\mu_{\perp} \rangle_e$ is that for the excited dipoles just after the excitation. The ratio between the two equals the ratio between the two dipole moments, $\langle \Delta\mu_{\perp} \rangle_e / \langle \Delta\mu_{\perp} \rangle_g = \mu/\mu_g$. In the derivation of eq 11, it was assumed that the equilibrium condition corresponds to $\langle \Delta\mu_{\perp} \rangle = 0$. The time resolution of the setup was insufficient to follow kinetics faster than 0.5 ns and left the only option: to analyze the signal amplitudes, $\langle \Delta\mu_{\perp} \rangle_{\text{max}}$, which can be calculated as:

$$\frac{1}{\langle \Delta\mu_{\perp} \rangle_{\text{max}}} = -\frac{1}{\langle \mu_{\perp} \rangle_e} \left(\frac{\tau_t}{\tau} + \left(\frac{\tau_t^2}{\tau^2} \right) \left(\frac{\mu}{\mu_g} - 1 \right) \right)^{1/(1-\tau_t/\tau)} \quad (12)$$

For the fitting of experimental variation of $\langle \Delta\mu_{\perp} \rangle_{\text{max}}$ with collision frequency using eq 12, one needs to know the intrinsic relaxation time, τ_r , in eq 9. As a first approximation, we will neglect its contribution ($\tau_t \ll \tau_r$) and presume $1/\tau = \xi k_{\text{col}} n$. Hence, there are three variables in the fitting: $\langle \mu_{\perp} \rangle_e$, product $\xi\tau_t$, and the ratio μ/μ_g . The latter is known from calculations and the experiments in solution:¹ $\mu/\mu_g \sim 10:7 = 1.4$, but its variation between 1 and 2 affects the outcome to no more than 30%. For example, in the range where $\langle \Delta\mu_{\perp} \rangle_{\text{max}}$ changes 5-fold, eq 12 can be roughly approximated as:

$$\frac{\langle \mu_{\perp} \rangle_g}{\langle \Delta\mu_{\perp} \rangle_{\text{max}}} \approx -a - b \frac{\tau_t}{\tau} \approx -a - b \tau_t \xi k_{\text{col}} n \quad (13)$$

Even though the linear approximation does not fit eq 12 well, it is more convenient for qualitative analysis. The best-fit coefficients a and b depend on the ratio μ/μ_g and the range of τ_t/τ variation so that the intercept a gets closer to the correct value of $a = -1$ for narrow ranges. For $\mu/\mu_g = 1.4$, the best-fit values are $a = 1.47$ and $b = 1.04$; they vary between $a = 1.35$ and $b = 1.28$ for $\mu/\mu_g = 1$ and $a = 1.51$ and $b = 0.71$ for $\mu/\mu_g = 2$. Thus, one can estimate the dipole moments and $\xi\tau_t$ by plotting the reciprocal of the dipole signal amplitude as a function of collision frequency:

$$\frac{1}{\langle \Delta\mu_{\perp} \rangle_{\text{max}}} \approx -\frac{a}{\langle \mu_{\perp} \rangle_g} - \frac{b \xi \tau_t}{\langle \mu_{\perp} \rangle_g} k_{\text{col}} n \quad (14)$$

Note that the intercept in eq 14 depends mostly on $\langle \mu_{\perp} \rangle_e$ (and $\langle \mu_{\perp} \rangle_g$), for which it provides a low limit estimate; finite τ_r would

increase its value. The same is true for original eq 12. The “slope” depends on $\langle\mu_{\perp}\rangle_e$, $\langle\mu_{\perp}\rangle_g$ and $\xi\tau_i$.

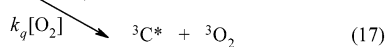
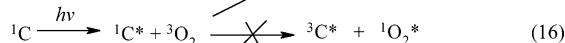
When fitted according to eq 12, the value of $\xi\tau_i$ varied between 0.6 ± 0.15 and 1.2 ± 0.2 ns for the N₂ pressure dependence (Figure 6B) and for the series of different gases at atmospheric pressure (Figure 6A), respectively. Here, again, $s = 50 \text{ \AA}^2$ was assumed, which corresponded to $k_{\text{col}} = 1.7 \times 10^6 \text{ s}^{-1} \text{ Torr}^{-1}$ (collision frequency $\nu_{\text{col}} = 1.1 \times 10^9 \text{ s}^{-1}$ at 670 Torr) for N₂ at room temperature. The dipole moment change was the same for both curves, $\langle\mu_{\perp}\rangle_e = 5.7 \pm 1.2 \text{ D}$.

The apparent difference in $\xi\tau_i$ between parts A and B of Figure 6 is not significant but may suggest that the collision efficiency factor ξ for diatomic gases is greater than those for monatomic gases. It is tempting to speculate that the difference is real and reflects a greater relaxation cross section for diatomic molecules, but currently there is not enough accuracy to make this claim.

In the above treatment, we presumed that the fluorescence lifetime of excited coumarin, τ_F , was independent of collisions. This assumption may not be correct, but currently there is no unambiguous approach for including it into our simplified model. The effect would not significantly alter our conclusions on the tilting time. Table 1 and Figure 3 suggest a possible increase of the lifetime, τ_F , with the frequency of collisions, which results from a competition between counteracting phenomena. On one hand, collisions induce vibrational relaxation to vibronic states with different Franck–Condon factors, from which the rates of radiative and nonradiative decay can be smaller. On another hand, angular relaxation of excited dipoles minimizes their optical coupling and the efficiency of stimulated emission,¹ making the lifetime of the excited state longer. As a first approximation, we neglected these effects for nitrogen and noble gases.

The situation clearly differed when oxygen gas was used. Because molecular oxygen is paramagnetic in its ground state, its presence induces intersystem crossing^{10,11} and results in formation of long-lasting triplet dipolar states, as illustrated in Figure 7. Aminocoumarins have a low intrinsic intersystem-crossing yield into the triplet state under ordinary conditions,^{6–9} and low yields of triplet formation were observed in inert gases as well. The yield of fluorescence quenching and the triplet yield increased in oxygen and depended on the frequency of collisions (pressure) with oxygen gas.

The following scheme represents competitive routes of deactivation for the singlet excited state of coumarin:



Coumarin fluorescence, with the rate constant k_F of reaction 15, competes with quenching via interconversion into the triplet state. The latter proceeds with the rate $k_q[\text{O}_2]$, according to reaction 17, while reaction 16 is not energetically feasible^{10,11} because the S–T gap in coumarin is smaller than the excited-state energy of $^1\text{O}_2^*$. Figure 7 demonstrates the dipole signals of covalently bound coumarin SAM and physisorbed coumarin 460 on quartz substrates in air and in oxygen. In both cases, two distinct components were observed: the “fast”, due to the short-lived singlet excited states, and the “slow”, due to the triplet states. The phenomenon is very similar to the previously observed effect of oxygen-induced intersystem crossing in solutions.^{10,11} The decay time of the slow component should

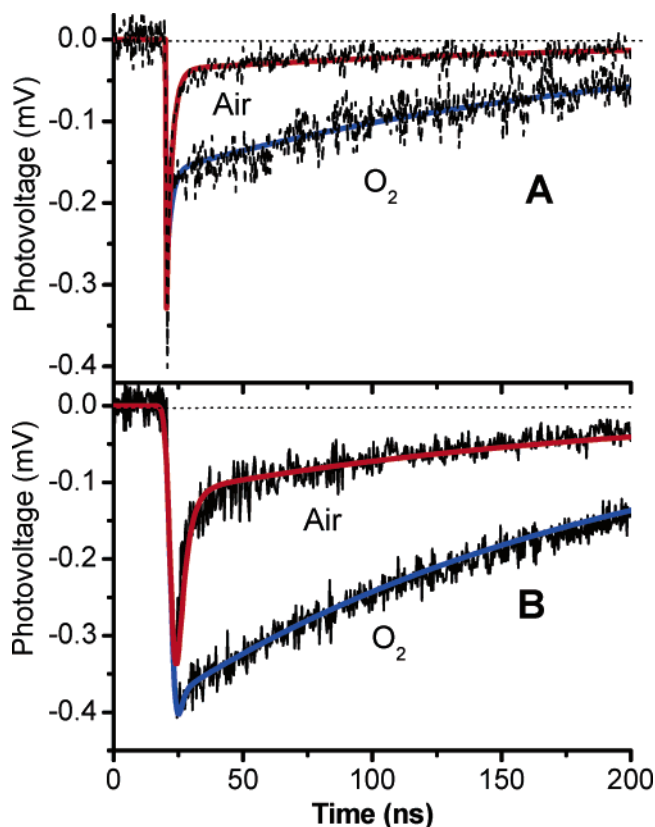


Figure 7. (A) SPTDC photovoltage signals from coumarin SAM on quartz in air and in flow of pure oxygen (670 Torr) after excitation by 416 nm. The best-fit curves correspond to $\tau_F = 0.5$ ns, and $\tau_{\text{isc}} = 2.4$ and 14 ns, for pure oxygen and air, respectively. (B) The same for physisorbed on quartz coumarin-460 in air and in pure oxygen after excitation with nitrogen laser at 337 nm. The best-fit curves were calculated with $\tau_F = 4.3$ ns, and $\tau_{\text{isc}} = 2.4$ and 14 ns for pure oxygen and air, respectively. In all cases, the signals were fitted with $\tau_{\text{RC}} = 173$ ns, corresponding to overall capacitance of 8.7 pF, almost equally split between calculated cell capacitance and stray capacitance, $C_s = 4.3$ pF.

be equal to the RC time of the circuit calculated using eq 3. The experimental value, given in the fit, agreed well with the calculated one using the cell capacitance and stray capacitance of 4.3 pF. Because stray capacitance affects not only the RC time but the value of the dipole moment change as well, this agreement corroborates the correctness for obtained values of $\langle\Delta\mu_{\perp}\rangle$.

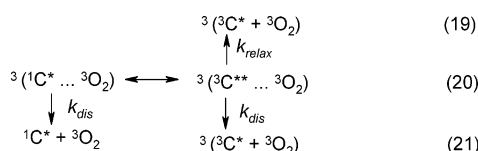
The increasing contribution of the slow component for dipole signals with oxygen partial pressure in Figure 7 was a direct result of increasing triplet yield, φ_T , induced by intersystem crossing via collisions with oxygen:

$$\varphi_T = \frac{1}{1 + (\tau_F k_q [\text{O}_2])^{-1}} \quad (18)$$

Different fluorescence lifetimes, τ_F , result in different magnitudes of the slow component in the dipole signal. If the dipole moment of the triplet state is the same as for the singlet excited state,^{6–9} the rate constant of intersystem crossing, k_q , can be obtained from φ_T . The observed apparent difference in the triplet yield for two coumarins correlates well with the difference in their singlet excited-state lifetimes, τ_F , in accordance with eq 18. For short-lived excited coumarin B molecules, deactivation via fluorescence prevailed over the intersystem crossing, while coumarin 460 experienced greater intersystem crossing yield for the same collision rates with oxygen.

Covalently bound coumarin B and coumarin 460 are similar in size and electronic structure and thus are expected to have similar rate constants, k_q . Indeed, $k_q = 6 \times 10^5 \text{ s}^{-1} \text{ Torr}^{-1}$ were observed for both, which is smaller than k_{col} calculated using eq 10. The ratio, $k_q/k_{\text{col}} \sim 0.35$, is close to the anticipated value of $k_q/k_{\text{col}} = 0.5$ that was previously found for intersystem crossing induced by free radical spin scramblers such as oxygen.^{11,12} In that mechanism, radicals induce S–T transitions in a charge transfer excited state by mixing their spin states in accordance with reactions 19–21.

The process originates in the formation of a transition state complex, $^3(\text{C}^* \cdots \text{O}_2)$ between the intramolecular charge transfer excited state, $^*\text{C}$, and a radical, oxygen in this case, in the overall triplet state. Different interaction between spins of the radical with charges in the excited state promotes spin-allowed transition in the complex with coumarin changing from its singlet, $^1\text{C}^*$, to triplet, $^3\text{C}^{**}$, state, as shown in reaction 20. Two asterisks in $^3\text{C}^{**}$ refer to an excess vibrational energy in the triplet state. If vibrationally excited triplet state, $^3\text{C}^{**}$, relaxes (reaction 19) faster than oxygen escapes from the complex (reaction 21), then all complexes follow reaction 19 and the overall intersystem crossing rate becomes equal the rate of collisions. When dissociation with the rate constant k_{dis} is faster than relaxation, k_{relax} , only half of $^1\text{C}^*$ end up as $^3\text{C}^*$.



Experimental rate constants were even less than the estimated half of the collision rate constant, $k_q/k_{\text{col}} \sim 0.35$. This observation suggests a very brief encounter between coumarin and gaseous oxygen, where not only is $k_{\text{dis}} \gg k_{\text{relax}}$, but the equilibrium in reaction 20 does not fully develop either. This can easily happen in the gas-phase reaction between coumarin and O_2 . Charge separation in coumarins is small, and the zero-field splitting between singlet and triplet states is large and anisotropic. In such a case, brief collisions may not be sufficient for a full coupling with all three triplet sublevels (T_{xx} , T_{yy} , T_{zz}), but only with one or two closest in energy. The estimated k_{col} is sensitive to the choice of the collision cross-section, s , and experimental k_q also bears a limited accuracy; thus their ratio has to be taken cautiously. Nevertheless, it seems unquestionable that k_q is measurably less than k_{col} ; whether it is by a factor of 2 or more requires further investigation.

In the last part, we will comment on the two parameters that we have not yet estimated. They are the tilting time, τ_t , and the number of molecules involved in formation of the dipole signal in gases. A more systematic interpretation of the discussed phenomenon would require evaluation of the generic Langevin equation for a one-dimensional rotor with the moment of inertia, I , rotating on angle θ around its axis as given by:¹⁵

$$I \frac{d^2\theta}{dt^2} = -\frac{\partial V}{\partial \theta} - \zeta \frac{d\theta}{dt} + \xi(t) \quad (22)$$

Here, ζ is the friction constant, and $\xi(t)$ is stochastic torque due to fluctuations. The moment of inertia, I , depends on the molecular mass, M :

$$I = MR^2 \quad (23)$$

and the linker length, R , which is measured from the molecule's

center of mass to the point of its attachment to the surface. If only random thermal motion with friction is considered, the solution of eq 22 can provide the information on the variation of the second moment of distribution:¹⁵

$$\langle \theta^2 \rangle = \frac{2k_B T}{\zeta} \left[t - \frac{I}{\zeta} (1 - e^{-\zeta t/I}) \right] \quad (24)$$

which for short times, $t \ll I/\zeta$ reduces to:

$$\langle \theta^2 \rangle = k_B T t^2 / I \quad (25)$$

and for long times, $t \gg I/\zeta$ simplifies to:

$$\langle \theta^2 \rangle = 2k_B T t / \zeta \quad (26)$$

Equation 25 allows estimation of the free inertial rotation time of a molecule as:

$$\tau_1 = \sqrt{\frac{MR^2}{k_B T}} \quad (27)$$

For $R \sim 9 \text{ \AA}$ and the mass of coumarin with the linker, $M \sim 380 \text{ g/mol}$, the estimated inertial rotation time is, $\tau_1 \sim 10 \text{ ps}$. Obviously τ_1 is too short to be the tilting time, τ_t , in our case. The dipoles do not move freely, but rather drift with some friction on a potential $V(\theta)$ that appears due to interaction with surrounding dipoles.

Orientation of the ground-state dipoles is in dynamic equilibrium characterized by some intrinsic frequencies of librations near the energy minima. When dipole–dipole interaction exceeds thermal energy, these librations involve simultaneous movement of a few molecules. Transitions between different minima happen on a longer time scale than the libration period. In the point dipole approximation, the minimum energy orientation for the ensemble corresponds to antiferroelectrical coupling in the surface plane¹⁶ with no component of the dipole moment perpendicular to the surface. Hindrance imposed by the molecules' finite size and corresponding van der Waals interactions between them and the surface, as well as intramolecular conformational impediments, produce nonzero perpendicular dipole orientation. The same hindrance is responsible for making the “tilting” time, τ_t , exceed the inertial rotation time, τ_1 , and contributes to reorienting dipoles back to their original assembly after excited molecules relax to the ground state.

In the limit of a dampened rotor, the terms for angular acceleration and stochastic torque in eq 22 can be neglected, and it reduces to:

$$\zeta \frac{d\theta}{dt} = -\frac{\partial V}{\partial \theta} \quad (28)$$

To solve eq 28, one needs to know the form of potential, $V(\theta)$, and the friction coefficient, ζ . Expressed as a function of angle, θ , from the normal, the dipole–dipole interaction per molecule is a result of averaging eq 7 over distances and angles in the surface plane:

$$V_{\text{d-d}}(\theta) = \frac{\mu^2}{r^3} [\alpha + \beta \cos^2 \theta] \quad (29)$$

where r is the average distance between molecules with dipole moment μ . Parameters α and β depend on the dipole distribution, e.g., the type of lattice they are arranged in. The minimum energy on this potential corresponds to $\theta = 90^\circ$, but finite

molecular sizes prevent it by contributing a counteracting repulsive interaction. The leading term of the lowest power of angular dependence should be proportional to $\sin^3 \theta$ such that the minimum energy angle, at which the two terms negate each other, can be identified. This angle is most likely close to the average angle obtained from absorption spectra ($\theta_{av} \sim 65^\circ$). The overall potential, $V(\theta)$, for $\theta > \theta_{av}$ appears fairly flat if only the $\sin^3 \theta$ term is included. Upon photoexcitation, the dipole–dipole interaction increases, while the other term remains almost the same. As a result, one can simplify the treatment in the vicinity of θ_{av} by considering the changed potential, $V_e(\theta)$, in eq 28 as due to the increased dipole moment:

$$V_e(\theta) = \mu_g^2 \frac{\mu_g}{r^3} [\alpha + \beta \cos^2 \theta] \quad (30)$$

After substituting eq 30 into eq 28, one recovers a pseudo-first-order decay of the dipole projection, $\cos \theta$, in the vicinity of θ_{av} :

$$\frac{d(\cos \theta)}{dt} = -\frac{2\beta\mu_g\mu \sin^2 \theta}{r^3\zeta} \cos \theta \approx -\frac{2\beta\mu_g\mu \sin^2 \theta_{av}}{r^3\zeta} \cos \theta = -\frac{\cos \theta}{\tau_t} \quad (31)$$

The tilting time:

$$\tau_t \sim \frac{r^3\zeta}{2\mu_g\mu} \quad (32)$$

appears to depend on the dipole moment values, their separation (i.e., the surface density), and the friction coefficient. However, this appearance may be deceiving because ζ has a significant contribution from dipole friction that is opposite in its dependence on μ and r .¹⁷

The amplitude of $\langle \Delta\mu_{\perp} \rangle_{\max}$ was quite large (and even larger $\langle \Delta\mu_{\perp} \rangle_e = 5.7 \pm 1.2$ D from the fit). Its value was not only greater than the amplitude of the positive going signal measured in solutions¹ but, more remarkably, larger than what is possible by tilting a single dipole. Indeed, presuming a complete tilting of an excited dipole, i.e., $\langle \cos \theta \rangle_{\text{exc}} = 0$, from eq 4 one gets $\langle \Delta\mu_{\perp} \rangle_g = -\mu_g \langle \cos \theta \rangle_g$, which, for the average angle $\theta_{av} = 65^\circ$ with respect to the normal ($\cos^2 \theta_{av} = \langle \cos^2 \theta \rangle_g = 0.18$) and $\mu_g = 7$ D, amounts to the amplitude of $\langle \mu_{\perp} \rangle_{\max}$ less than 3 D. Moreover, the magnitude of the experimental value of $\langle \mu_{\perp} \rangle_e$ was obtained under the assumption of no intrinsic rotational relaxation, $1/\tau_r = 0$, and thus was a low limit estimate. The value of $\langle \mu_{\perp} \rangle_{\max}$ greater than 3 D can be achieved only if more than one dipole experience tilting. If the tilting of the excited molecule is incomplete ($\theta_{\text{exc}} < 90^\circ$), then even greater number of neighboring molecules would be required to gain the negative signal of the appropriate amplitude. All of these observations suggest that the signal arises from tilting of more than one molecule, as would be expected for strongly interacting dipoles. Dipole–dipole interaction calculated using eq 7 declines dramatically with distance and already becomes less than $k_B T$ at the second layer of neighbors from the excited dipole for our surface densities, i.e., more than 12 Å away. That allows us to make a conservative estimate for the number of ground-state molecules involved in tilting as only 3–5. For that number of molecules involved in the dipole signal formation, their additional tilting angle toward the surface can be below 10° ,

which is not dramatic. It would be helpful to correlate the dipole signal with surface concentration of dipoles, but unfortunately, it was not feasible. Sensitivity limitations would not allow a significant concentration decrease, which is also ambiguous. The procedure of covalent immobilization requires appropriate treatment of “empty” sites on the surface. Either in the form of unreacted amines or “terminated” by other molecules, these sites would affect not only the interaction between coumarins but with the surface as well. We plan to address this in future studies.

Conclusions

We have demonstrated that the surface-assisted photoinduced transient displacement charge (SPTDC) technique, when applied to small molecules that were covalently immobilized on flat surfaces, had a significant contribution from molecular rotation. The effect was mostly profound in gaseous media, where the dipole signal from a dense monolayer of dipolar molecules, such as coumarin, became opposite in sign to that observed in solution. The phenomenon was primarily attributed to dipole–dipole interaction between molecules in the monolayer. Increasing dipole moment of photoexcited coumarin and inducing stronger dipole–dipole interaction results in reorientation (tilting) of molecules toward the surface. The signal amplitude declined with increasing the rate of collisions, suggesting that collision-induced relaxation impeded the tilting. This allowed for the estimation of tilting time for covalently bound coumarin, on the order of 1 ns, which is much slower than the inertial rotation time of a single molecule.

When oxygen was used as a gaseous medium, an additional relaxation pathway with formation of the long-lived triplet state of coumarin was observed; the rate constant of the latter was less than the collision rate with oxygen molecules.

Acknowledgment. The project was supported in part by the grants from the Research Corporation and the National Institutes of Health (NIH SCORE GM08136). We are grateful to Charles Braun, David Smith, and Ivan Vlasiouk for inspiring discussions.

Supporting Information Available: Derivation of eqs 11–14 and 30–32. This material is available free of charge via the Internet at <http://pubs.acs.org>.

References and Notes

- (1) Krasnoslobodtsev, A.; Smirnov, S. *J. Phys. Chem. A*, **2006**, *110*, 17931.
- (2) Krasnoslobodtsev, A.; Smirnov, S. *Langmuir* **2001**, *17*, 7593.
- (3) Krasnoslobodtsev, A.; Smirnov, S. *Langmuir* **2002**, *18*, 3181.
- (4) Smirnov, S. N.; Braun, C. L. *Rev. Sci. Instrum.* **1998**, *69*, 2875.
- (5) *HyperChem Pro* version 7.5; Hypercube, Inc.: Gainesville, FL, 2003.
- (6) Moylan, C. R. *J. Phys. Chem.* **1994**, *98*, 13513.
- (7) Sahyun, M. R. V.; Sharma D. K. *Chem. Phys. Lett.* **1992**, *189*, 571.
- (8) Lewis, J. E.; Maroncelli, M. *Chem. Phys. Lett.* **1998**, *282*, 197.
- (9) Samanta, A.; Fessenden, R. W. *J. Phys. Chem. A* **2000**, *104*, 8577.
- (10) Smirnov, S.; Vlasiouk, I.; Kutzki, O.; Wedel, M.; Montforts, F. *P. J. Am. Chem. Soc.* **2002**, *124*, 4212.
- (11) Vlasiouk, I.; Smirnov, S.; Kutzki, O.; Wedel, M.; Montforts, F. *P. J. Phys. Chem. A* **2002**, *106*, 8657.
- (12) Smirnov, S. N.; Braun, C. L. *Chem. Phys. Lett.* **1994**, *217*, 167.
- (13) Smirnov, S. N.; Braun, C. L. *J. Phys. Chem.* **1994**, *98*, 1953.
- (14) Tadjikov, B.; Krasnoslobodtsev, A.; Smirnov, S. *Phys. Chem. Chem. Phys.*, in preparation.
- (15) Reif, F. *Fundamentals of Statistical and Thermal Physics*; McGraw-Hill: New York, 1965; p 566.
- (16) Rozenbaum, V. M. *Phys. Rev. B* **1996**, *53*, 6240.
- (17) Nee, T.-W.; Zwanzig, R. J. *Chem. Phys.* **1970**, *52*, 6353.